Effective Deformation Potential in Ultrathin SOI

T, Tanaka, and K. M. Itoh
School of Fundamental Science and Technology, Keio University, Yokohama 223-8522, Japan
e-mail: tt112157@z7.keio.jp

INTRODUCTION

Recent downsizing of Si MOSFETs face problems of short channel effects. To suppress these effects, ultrathin Silicon-on-Insulator (UTSOI) MOSFETs have attracted much attention. For bulk Si and bulk Si MOSFETs, deformation potentials (DPs) Ξ_d=1.1 eV and Ξ_u=10.5 eV or simplified effective DP D_{ac}=12.0 eV have been used to calculate the relaxation time of intravalley acoustic phonon scattering [1,2]. However, increase of D_{ac} in UTSOI MOSFETs was experimentally reported recently [3]. There are still uncertainties of effective DP approximated from anisotropic DPs and elastic approximation of intravalley acoustic phonon scattering in UTSOI MOSFETs. Thus, it is important to validate the DPs Ξ_d=1.1 eV and Ξ_u=10.5 eV to apply nanoscale devices. In this paper, we report the calculation of effective DPs from the anisotropic values (Ξ_d=1.1 eV and Ξ_u=10.5 eV) in UTSOI MOSFETs.

CALCULATION

Before the calculation of effective DPs, mobility in the bulk Si MOSFET was calculated to check our simulation. Parabolic subband structures were calculated by self-consistent solver of one-dimensional Poisson and Schrödinger equations. Then, transition probabilities and transport relaxation times were obtained from Fermi's Golden rule. For four-fold degenerated valleys, transport relaxation times in the same constant energy surface were approximated by same value. Acoustic phonons, surface optical phonons and surface roughness were considered as intravalley scatterings [4]. Three f-type and three g-type phonon scatterings were included as intervalley scatterings [4]. Mobility was calculated from the energetically averaged transport relaxation time. Figure 1 shows the comparison between our simulation and experimental mobility [5]. Roughness parameters were Δ=0.51 nm and Λ=1.0 nm, and doping concentration was N_A =3.9×10^{15} cm^{-3}. Then, effective DPs in UTSOI MOSFETs were determined by comparing between two mobility calculated from anisotropic DPs and the effective DP. In addition to elastic scatterings, inelastic scatterings of intravalley acoustic phonons were also calculated by

$$W(E_i)=\frac{2\pi}{\hbar}\sum_{q,f,j}\frac{\hbar q^2}{2\rho V\omega_q}D_j(\boldsymbol{q})\left[N_q+\frac{1}{2}\mp\frac{1}{2}\right]$$

$$\times\left|\langle f|\exp(i\boldsymbol{q}\cdot\boldsymbol{r})|i\rangle\right|^2\delta(E_i\pm\hbar\omega_q-E_f),\quad(1)$$

where $W(E_i)$ is the transition probability at initial electron energy E_i, q is the magnitude of phonon wavevector, ρ is the mass density, V is the crystal volume, $\omega_q=s_jq+c_jq^2$ is the isotopically approximated phonon frequency, s_j (j=LA or TA) is the sound velocity, c_j is the constant in Ref. [6], $D_j(\boldsymbol{q})$ is the anisotropic DP, N_q is the phonon occupation factor, and i (f) represents the initial (final) state index. Figure 2 shows the calculated transport relaxation time of the first subband in the 6.0 nm UTSOI MOSFET. The surface inversion carrier concentration was N_S =4.0×10^{12} cm^{-2}. Using these result, mobility was calculated. Calculated mobility from anisotropic DP and empirical DP in Ref. [3], and experimental mobility in Ref. [7] were shown in Fig. 3. Finally, Fig. 4 shows obtained effective DPs.

SUMMARY

We calculated effective DPs in UTSOI MOSFETs from the anisotropic DPs with considering inelastic scatterings of intravalley acoustic phonon scatterings. Lower effective DP than empirical DP in Fig. 4 suggests the change of DPs in UTSOI MOSFETs. However, nonparabolicity of conduction band have not been included in calculations yet. Until the conference, we include this effect and improve our calculation.

978-3-901578-26-7 © 2013 Society for Micro- and Nanoelectronics

ACKOWLEDGEMENT

This work has been supported in part by the Grant-in-Aid for Scientific Research and Project for Developing Innovation Systems by CREST-JST.

REFERENCES

[1] M. V. Fischetti, and S. E. Laux, *Band structure, deformation potentials, and carrier mobility in strained Si, Ge, and SiGe alloys*, Journal of Applied Physics **80**, 2234 (1996).

[2] S. Takagi, J. L. Hoyt, J. J. Welser, and J. F. Gibbons, *Comparative study of phonon-limited mobility of two-dimensional electrons in strained and unstrainedSi metal-oxide-semiconductor field-effect transistors*, Journal of Applied Physics **80**, 1567 (1996).

[3] T. Ohashi, T. Takahashi, N. Beppu, S. Oda, and K. Uchida, *Experimental evidence of increased deformation potential at MOS interface and its impact on characteristics of ETSOI FETs*, IEDM Tech. Dig., 2011, pp. 16.4.1–16.4.4.

[4] M. V. Fischetti, and S. E. Laux, *Monte Carlo study of electron transport in silicon inversion layers*, Physical Review B **48**, 2244 (1993).

[5] S. Takagi, A. Toriumi, M. Iwase, and H. Tango, *On the universality of inversion-layer mobility in Si MOSFETs. Part I-Effect of substrate impurity concentration*, IEEE Transactions of Electron Devices **41**, 2357 (1994).

[6] E. Pop, R. W. Dutton, and K. E. Goodson, *Analytic band Monte Carlo model for electron transport in Si including acoustic and optical phonon dispersion*, Journal of Applied Physics **96**, 4998 (2004).

[7] K. Uchida, J. Koga, and S. Takagi, *Experimental study on electron mobility in ultrathin-body silicon-on-insulator metal-oxide-semiconductor field-effect transistors*, Journal of Applied Physics **102**, 074510 (2007).

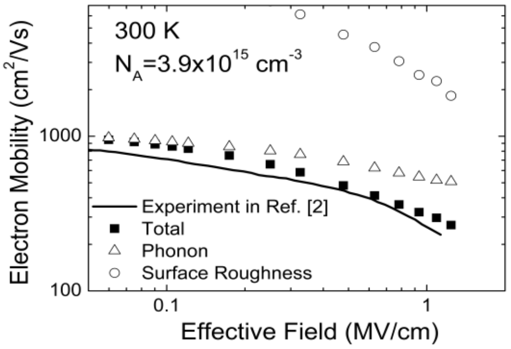

Fig. 1. Comparison between experimental (solid line Ref. [5]) and simulated mobility in bulk Si MOSFET.

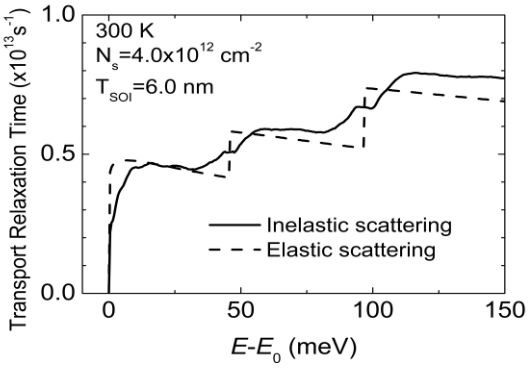

Fig. 2. Calculated transport relaxation times of the first subband.E-E_0 is the energy from the bottom of the subband.

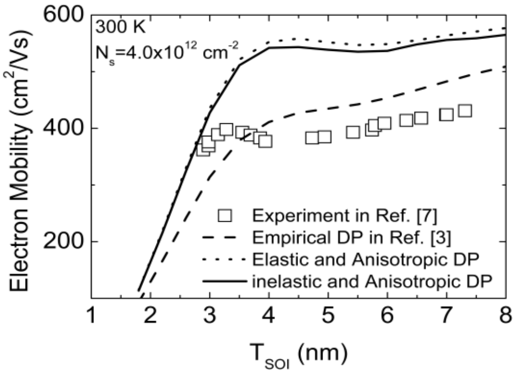

Fig. 3. Comparison between experimental (blank square Ref. [7]) and simulated mobility in UTSOI MOSFETs.

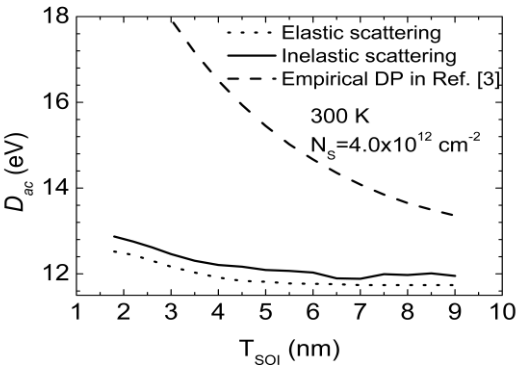

Fig. 4. Comparison between empirical DP in Ref. [3] and effective DPs calculated from elastical and inelastical intravalley acoustic phonon scattering.